L. Horny, H. Chlup, J. Kronek, E. Gultova, L. Heller, R. Zitny and D. Vokoun (2011) **Inflation-Extension Test of Silicon Rubber-Nitinol Composite Tube**. *IFMBE Proceedings* 37:1027-1030. DOI: 10.1007/978-3-642-23508-5_267 Manuscript version.

Inflation-extension test of silicon rubber-nitinol composite tube

L. Horny[1], J. Kronek[1], H. Chlup[1], E. Gultova[1], L. Heller[2], R. Zitny[3], and D. Vokoun[2]

[1] Department of Mechanics, Biomechanics and Mechatronics, Faculty of Mechanical Engineering of the Czech Technical University in Prague, Prague, Czech Republic

[2] Institute of Physics, Academy of Sciences of the Czech Republic, Prague, Czech Republic

[3] Department of Process Engineering, Faculty of Mechanical Engineering of the Czech Technical University in Prague, Prague, Czech Republic

Abstract— **Composite tube fabricated from elastomer matrix reinforced with NiTi wires was tested within simultaneous inflation and extension. Four different longitudinal weights were applied (m=41g; 188g; 488g; and 785g) to induce initial prestrain of the tube. The inflation was induced with repeating pressurization up to 200kPa; four times with each weight. Displacements and loading pressure were recorded into PC.**

No significant hysteresis and material instability, typical for elastomeric tubes, were observed. Simplified model, assuming the tube to be anisotropic hyperelastic continuum, was adopted in order to estimate material parameters by analytical model of the thick-walled vessel. This model was only successful in fitting the data corresponding to the smallest longitudinal weight.

It was concluded that NiTi reinforcement reduces elastomer viscoelasticity in macroscopic response, which can not be fully described with the model considering the effect of wires only as the introduction of anisotropy.

Keywords— **anisotropy, composite material, hyperelasticity, inflation-extension test, Nitinol.**

I. Introduction

Structures based on thin NiTi wires have become increasingly utilized in biomedical engineering products and devices. They are much attractive due to extraordinary material properties of Nitinol (roughly equi-atomic nickel-titanium alloy). So-called *shape memory*, *superelasticity* and good *biocompatibility* are the most important of them [1,2]. Nitinol is especially used in a production of self-expandable stents. They usually stand as distending scaffolds which restore the delivery of a medium through narrowed segments of conduits (blood flow in arteries, food in esophagus) [1,3]. Prior to medical treatment NiTi structure is metallurgically programmed to operating shape and deformed to small dimensions required within the intraluminal implantation. Subsequently it is delivered with a catheter into the target location where a shape constrictor is removed and the stent expands itself.

This expansion, which involves large strains, is possible due to Nitinol superelasticity [1,4-6]. Strain-induced phase transformation (martensite-austenite) endows NiTi material with unusual recoverable deformation capacity (elongation higher than 10% can be achieved). Because Nitinol wires are processible by common textile technologies these properties (shape memory, superelasticity) may also be utilized within designing outside the biomedical engineering. Here, especially new designs of hydraulic valves or pumps with NiTi membranes might be taken into consideration.

Such a membrane would require an implementation of NiTi wires into any compliant matrix. Up to date scientific literature reports few examples of NiTi wire-polymer matrix composites [7-9]. In contrast to biomedical applications, this area, however, still remains somewhat unexplored.

The aim of the present study is to investigate mechanical response of the elastomeric tube reinforced with thin NiTi wires. Pressure-diameter and longitudinal extension-force relationships were obtained within the inflation-extension test with the silicon rubber tube with implemented NiTi braided structure. This is only the pilot study which can not report final conclusions and constitutive model of the structure which is composite in its nature. Nevertheless, preliminary results will direct us at suitable computational model.

II. Methods

A. Sample preparation

NiTi wire with a diameter 100 μm used in this study was purchased from Fort Wayne Metals (Indiana, USA). Tubular sample of silicon elastomer-NiTi wire composite was fabricated at the Institute of Physics of the Czech Academy of Sciences. Metallic part of the final composite was fabricated as fenestrated cylindrical shell (braided structure of NiTi fibers) with 36 helically coiled wires; see Fig. 1. Wires were wound around in two families of helices symmetrically disposed along the longitudinal axis of the cylinder with the pitch angle approximately ±58° (measured between circumferential axes-helix). Tubular NiTi structure was subsequently annealed at 450°C for 30 minute. Mechanical properties of the wire are summarized in Table 1. For detailed description of the mechanical behavior of the Nitinol wires see [5,6].

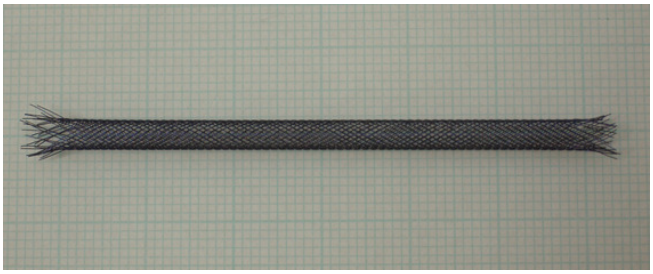

Figure 1 Braided Nitinol structure before polymer infiltration. There are 36 wires wounded around in two families of helices with the pitch angle approx. ±58°.

Used polymer matrix belongs to the group of silicon elastomers (trademark Sylgard 160) obtained as the mixture of soft and hard phase (volume ratio 1:1). NiTi textile-polymer composite sample was prepared by infiltration of braided structure laid in a mold with the polymer and hybridizing it by curing at room temperature for 24 hours. Final composite vessel, shown in Fig. 2, had outer and inner radius equal to R_o=3.025mm, and R_i=1.25mm, respectively.

B. Inflation-extension test

In order to obtain mechanical response of the sample the inflation-extension test was carried out in the Laboratory of Human Biomechanics, Faculty of Mechanical Engineering of the Czech Technical University in Prague.

Table 1 Summary of the sample.

NiTi wire		
Young modulus of austenite	46.2	GPa
Young modulus of martensite	18.0	GPa
Transformation yield stress of austenite at 20°C	0.553	GPa
Maximum recoverable transformation strain	5.23	%
Ultimate tensile strength	1.67	GPa
Yield stress	1.48	GPa
Strain at failure	14.2	%
Pseudoelastic stress hysteresis	0.34	GPa
Wire thickness	0.1	mm
Sylgard 160		
Approx. linear behavior in tension with Young modulus	1.7	MPa
Composite structure		
Reference outer radius of the silicon-NiTi tube	3.025	mm
Reference inner radius of the silicon-NiTi tube	1.250	mm
Number of helices	36	—
Helix angle (declination from circumferential axis)	±58	°
Reference radius of the NiTi shell	1.75	mm

Within the inflation-extension test the sample is loaded by internal pressure and axial force. The force is originated by the pressure which is applied to the end of the tube (closed tube configuration) and with additional weight. This is called the total axial force *N*. The experimental setup is documented in Fig. 2. The pressurization was carried out manually by a syringe. Four different weights were consecutively applied to induce longitudinal prestrain; *m*=41g; 188g; 488g; and 782g (*m* is the total mass of the longitudinal load under zero transmural pressure). Four pressurization cycles were repeated with each weight.

Displacements of the inflated tube were recorded by point optical probes Chrocodile M4 (Precitec Group, Germany). Two of these sensors were involved in the longitudinal displacement and torsion angle measurement. The change of the diameter was recorded with the laser scanner ScanControl LLT 2800-25 (Micro-epsilon, Germany). The internal pressure was monitored with the pressure transducer Kulite XLT-123B-190M-3.5BAR-D (Kulite Semiconductor Products, USA). All quantities were recorded into a PC for further post-processing.

C. Model

Several assumptions were made in order to keep simplicity necessary for analytical treatment of the problem. The material of the final structure was homogenized. It means that reinforcement wires were considered to define preferred directions in hyperelastic continuum. Thus, their influence was reduced to the originating anisotropy. Both families of wires were presumed to be mechanically equivalent. It results in so-called locally orthotropic material [10] (chapter 6). Viscoelastic properties of the silicon rubber were neglected due to the reinforcement with the stiff elastic fibers.

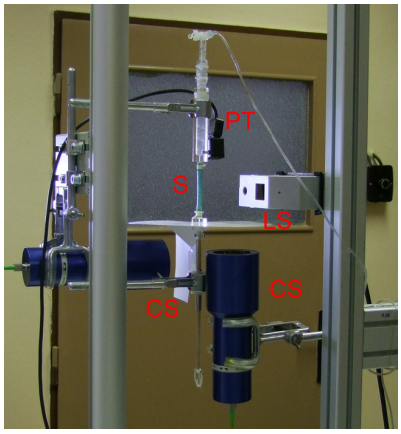

Figure 2 Experimental setup: S – sample; PT – pressure transducer (Kulite); LS – laser scanner (Micro-epsilon); CS – confocal sensor (Precitec).

L. Horny, H. Chlup, J. Kronek, E. Gultova, L. Heller, R. Zitny and D. Vokoun (2011) **Inflation-Extension Test of Silicon Rubber-Nitinol Composite Tube**. *IFMBE Proceedings* 37:1027-1030. DOI: 10.1007/978-3-642-23508-5_267 Manuscript version.

The strain energy density function W was considered to be decoupled into isotropic part (Mooney-Rivlin; elastomer contribution) and anisotropic part (contribution of the wires). W is defined in (1).

$$W = \frac{\mu}{2}(I_1 - 3) + \frac{\nu}{2}(I_2 - 3) + c(I_4 - 1)^2 \quad (1)$$

Here μ, ν, and c denote stress-like material parameters. I_1 and I_2 are the first and the second principal invariant of the right Cauchy-Green strain tensor $\mathbf{C}$. It can be written as $\mathbf{C}=\mathbf{F}^T\mathbf{F}$, where $\mathbf{F}$ is the deformation gradient. I_4 denotes additional invariant generated by anisotropy of the continuum.

Considering simultaneous extension and inflation of incompressible tube (due to rubbery matrix) $\mathbf{F}$ is obtained as $\mathbf{F}=\mathrm{diag}[RL/(rl), r/R, l/L]=\mathrm{diag}[\lambda_R, \lambda_T, \lambda_Z]$. Here R and L denote radius and length in the reference configuration. Lowercase letters indicate spatial configuration. It results in $I_4=\lambda_T^2\cos^2(\beta)+\lambda_Z^2\sin^2(\beta)$. Mention that mechanical equivalency of two families of reinforcing fibers implies that one helical family is disposed under β and second one under $-\beta$; here considered as the declination from circumferential direction. Details of this approach can be found in [11], and [12]. Also equilibrium equations for the inflated and extended thick-walled cylindrical tube were adopted from the latter. Thus observed internal pressure, p, and longitudinal load, N, can be predicted via (2) and (3).

$$p = \int_{\lambda_o}^{\lambda_i} \frac{1}{\lambda_T^2\lambda_Z - 1}\frac{\partial W}{\partial \lambda_T} d\lambda_T \quad (2)$$

$$\frac{N}{\pi R_i^2} = \left(\lambda_i^2\lambda_Z - 1\right)\int_{\lambda_o}^{\lambda_i} \frac{1}{\left(\lambda_T^2\lambda_Z - 1\right)^2}\left(2\lambda_Z\frac{\partial W}{\partial \lambda_Z} - \lambda_T\frac{\partial W}{\partial \lambda_T}\right)\lambda_T d\lambda_T + p\lambda_i^2 \quad (3)$$

Here, in equations (2) and (3), W has to be considered after eliminating λ_R via incompressibility constraint; $\lambda_R=1/(\lambda_T\lambda_Z)$. Because the inflation is modeled by means of the thick-walled tube the integration is computed over $\lambda_T\in[\lambda_T(R_o)=\lambda_o; \lambda_T(R_i)=\lambda_i]$. We note that the aspect ratio $R_i/(R_o-R_i)=0.7$.

III. Results

Data sample intended for parameters estimation was collected from the last pressurization cycle of each longitudinal load. It is shown in Fig. 3. Pressure-circumferential stretch relationships suggest that macroscopic response of the sample holds the behavior typical for inflated polymer tube (concave curve). No material instability (non-uniform bulge), however, was observed. Implemented wired structure probably prevents the tube from it. Observed small torsions (0-2.5°/5cm) were not considered to be materially intrinsic (not depicted).

Material parameters were estimated using weighted least square optimization in Maple 13 (Maplesoft, Canada). They are listed in the caption of Fig. 3. However, it has to be said that the model (1) failed in the prediction of entire range of the experiment. Only data for the first longitudinal weight were fitted successfully. Especially longitudinal load was dramatically underestimated (error reached up to ≈5.5N at the peak value). It aimed us to fit data corresponding to the first weight (m=41g) separately. This result is depicted with continuous curves in Fig. 3.

On the basis of general constitutive equation for hyperelastic incompressible material, $\sigma_{jk}=\mathrm{F}_{jk}\partial W/\partial \mathrm{F}_{jk}-P\delta_{jk}$, σ_{tt} (circumferential) and σ_{zz} (axial) were computed. Corresponding stress-stretch curves are depicted in Fig. 4. This is the constitutive behavior of the homogenized material.

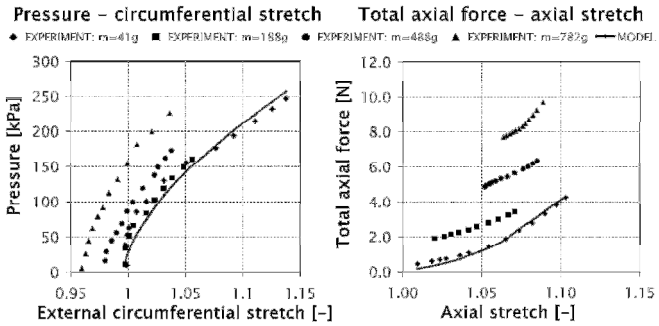

Figure 3 Observation points fitted with the model (1); estimated parameters: μ=-18.37kPa; ν=220.9kPa; c=34.62kPa; and β=0. The predictions only for m=41g are included.

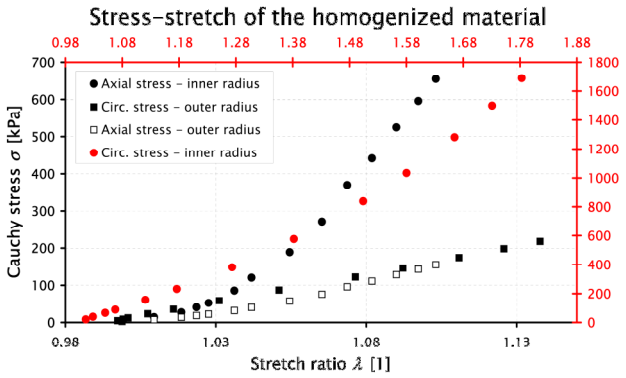

Figure 4 (Cauchy) Stress-stretch relationships resulting from the inflation-extension of the tube under m=41g for inner and outer radius. We note that $\sigma=\sigma(\lambda_T,\lambda_Z)$. In this graph, however, stress-stretch relationships in 2D are depicted. It means that, if one considers vertical axis as circumferential stress at the inner radius, horizontal axis must be read as the circumferential stretch ratio (at the inner radius). The axial stress also follows this rule; σ_{zz}-λ_Z are depicted. Material parameters are listed in Fig. 3.

IV. Discussion and conclusion

Our study aims to the modeling of inflation-extension behavior of NiTi-elastomer composite tube. It was concluded that NiTi reinforcement reduces elastomer viscoelasticity in macroscopic response (negligible hysteresis was observed), which can not be fully described with the model considering the effect of wires only as the introduction of anisotropy (only one longitudinal weight from four was fitted successfully).

There are several potential sources of errors and oversimplifications. As first, any debonding, resulting in delamitanion, might occur within the experiment. Unfortunately, at present time no inspection method suitable for this purpose is available for us. This effect can be presented as pull-out of implemented wires. It especially may be expected at the fixation places of the specimen (cannulas connecting the specimen into the pressurization setup). However, braided structure of Nitinol wires rather resists itself against the pull-out due to the presence of cross-points in the structure.

Also homogenization itself is somewhat problematic; especially when stiff NiTi wires are combined with the compliant polymer matrix. This procedure leads to unrealistic values of the deformation. As shown in Fig. 4, homogenized model sustains stretches up to 1.75 in the circumferential direction at the inner radius of the tube. It calls for structural model separating responses of the constituents. It is, however, beyond the scope of this study, which is intended to be only preliminary report.

Regardless to above mentioned one conceptual problem remains. Anisotropic invariant I_4 measures curved extension of the reinforcing wires. But it is questionable if it is correct in case of Nitinol wire. Its deformation behavior is probably much more spring-like than fiber-like. Present model, for the sake of simplicity, does not reflect this phenomenon. The incorporation of bending (or torque) stiffness probably will improve the model. Recently derived theory of fibers with bending stiffness [13], strictly based on invariant formulation, seems to be attractive. It is especially promising with respect to analytical treatment of the problem employed herein, because structural models of fiber-matrix kinematics (or interaction) usually necessitate finite element analysis to be employed.

Acknowledgment

This work has been supported by projects of the Czech Ministry of Education MSM6840770012 and the Czech Science Foundation P108/10/1296.

References

1. Stoeckel D, Pelton A, Duerig T (2004) Self-expanding nitinol stents: material and design considerations. Eur Radiol 14:292–301 DOI 10.1007/s00330-003-2022-5
2. Mani G, Feldman MC, Patel D, Agrawal CM (2007) Coronary stents: materials perspective. Biomaterials 28:1689–1710 DOI doi:10.1016/j.biomaterials.2006.11.042
3. Duerig TW, Tolomeo DE, Wholey M (2000) An overview of superelastic stent design. Min Invas Ther Allied Technol 9:235–246
4. Kim JH, Kang TJ, Yu W-R (2008) Mechanical modeling of self-expandable stent fabricated using braiding technology. J Biomech 41:3202–3212 DOI 10.1016/j.biomech.2008.08.005
5. Heller L, Kujawa A, Šittner P, Landa M, Sedlák P, Pilch J (2008) Quasistatic and dynamic functional properties of thin superelastic NiTi wires. Eur Phys J Special Topics 158:7–14 DOI 10.1140/epjst/e2008-00646-6
6. Heller L, Vokoun D, Majtás D, Šittner P (2008) Thermomechanical characterization of shape memory alloy tubular composite structures. Advan Science Technol 59:150–155. DOI 10.4028 /www.scientific.net/AST.59.150
7. Neuking K, Abu-Zarifa A, Youcheu-Kemtchou S, Eggeler G. (2005) Polymer/NiTi-composites: fundamental aspects, processing and properties. Adv Eng Mater 7:1014–1023 DOI 10.1002/adem.200500130
8. Murasawa G, Tohgo K, Ishii H (2004) Deformation behavior of NiTi/Polymer shape memory alloy composites – experimental verifications. J Compos Mater 38:399–416 DOI 10.1177/0021998304040553
9. Jarali CS, Raja S (2008) Homogenization and pseudoelastic behavior of composite materials reinforced with shape memory alloy fibers. J Compos Mater 42:1685–1707 DOI 10.1177/0021998308092201
10. Holzapfel GA (2000) Nonlinear solid mechanics. John Wiley and Sons, Chichester
11. Holzapfel GA, Gasser TC, Ogden RW (2000) A new constitutive framework for arterial wall mechanics and a comparative study of material models. J Elast 61:1–48 DOI 10.1023/A:1010835316564
12. Ogden RW (2009) Anisotropy and nonlinear elasticity in arterial wall mechanics, in: Biomechanical Modelling at the Molecular, Cellular and Tissue Levels, CISM 508, pp 179–258, DOI 10.1007/978-3-211-95875-9_3
13. Spencer AJM, Soldatos KP (2007) Finite deformations of fibre-reinforced elastic solids with fibre bending stiffness. Int J Nonlin Mech 42:355–368 DOI 10.1016/j.ijnonlinmec.2007.02.015

Author: Lukas Horny
Institute: Faculty of Mechanical Engineering of the CTU in Prague
Street: Technicka 4
City: Prague
Country: Czech Republic
Email: lukas.horny@fs.cvut.cz